# DAΦNE BROAD-BAND BUTTON ELECTRODES

*F. Marcellini, M.  Serio, M.  Zobov*

## Introduction

The beam position monitor (BPM) system is the primary diagnostic system in the DAΦNE [1] main rings. We have 38 BPMs in each ring and 12 in the common part of the interaction regions. They consist of four "button" electrodes mounted flush with the vacuum pipe. In all of them the same type of electrode (SMA 50-MB from Ceramex, France) is used, but, since the vacuum chamber cross-section is largely variable along the ring circumference, we have developed several different designs with different values of the transfer impedance according to the vacuum chamber geometry.

In addition to the measurement of the stationary closed orbit, done with narrow-band detectors, we need other special button monitors to measure the individual time and x/y position offset, on a bunch by bunch basis, i.e.: without "memory" of the preceding bunch, in the front-end section of the longitudinal and transverse feedback systems. These monitors are to be placed in the non-intersecting straight sections.

The horizontal (vertical) offset is measured at two distinct locations ~ $\pi/2$ away in betatron phase, as the difference signal of two button electrodes, while the longitudinal offset is determined by comparing the sum signal of four button electrodes to an RF-synchronous clock at the 4th (30 bunches) or 6th (120 bunches) harmonic of the RF frequency of 368 MHz.

The total of such special button electrodes is 12 per ring. They must satisfy the following two requirements:
- to have a reasonably high transfer impedance $Z_b$, free from narrow-band resonances in the frequency range of utilization: the necessary design value for DAΦNE is $0.3 \div 0.4 \ \Omega$ in the region $1300 \div 2200$ MHz, to be compared to ~ $0.2 \ \Omega$ of the ordinary BPM electrodes in the same section;
- to keep the beam coupling impedance and parasitic losses within acceptably low values.

As a general rule, a design with higher transfer impedance has also higher coupling impedance. For example, both the transfer and coupling impedances grow very strongly with increase of the button radius. So, a compromise has to be found in order to satisfy the two conflicting requirements.

In this Note we describe the proposed button design and calculate its transfer and coupling impedances.

## 1. General Considerations

The button electrode is mainly sensitive to the beam electric field. The usual equivalent circuit representation of an electrostatic monitor is a current generator of the same value of the image current intercepted fraction, shunted by the electrode capacitance to ground. If the button is connected to the detector circuit by means of a short run of coaxial cable having characteristic impedance $R_0$ and terminated into an $R_0$ resistor, the transfer (signal) impedance for a centered beam, i.e. the complex ratio of the voltage induced by the beam at the external termination to the beam current, can be written as (see Appendix)

$$Z_b(\omega) = \phi R_0 \left( \frac{\omega_1}{\omega_2} \right) \frac{j\omega/\omega_1}{1 + j\omega/\omega_1} \,,$$

$$\mathbf{Re}\{Z_b(\omega)\} = \phi R_0 \left( \frac{\omega_1}{\omega_2} \right) \frac{(\omega/\omega_1)^2}{1 + (\omega/\omega_1)^2} \quad , \quad \mathbf{Im}\{Z_b(\omega)\} = \phi R_0 \left( \frac{\omega_1}{\omega_2} \right) \frac{(\omega/\omega_1)}{1 + (\omega/\omega_1)^2} \quad ,$$

(1)

where $\omega_1 = 1/R_0 C_b$ and $\omega_2 = c/2r$ (= 1/electrode traversal time), with $C_b$ the button capacitance to ground, r the button radius, c the speed of light, $\phi$ the *coverage factor* = r/4b and b the beam pipe radius.

The frequency response is of the high-pass type. We can recognize two regimes:

Low frequency ( $\omega \ll \omega_1$ )
$$Z_b(\omega) = \phi R_0 \frac{j\omega}{\omega_2} = j\omega R_0 \left( \frac{r^2}{2bc} \right).$$
(2)

High frequency ( $\omega \gg \omega_1$ )
$$Z_b(\omega) = \phi R_0 \left( \frac{\omega_1}{\omega_2} \right) = \frac{r^2}{2bc\, C_b} \,.$$
(3)

In the low frequency regime the electrode acts like a time differentiator. The transfer impedance is largely independent on the value of the capacitance $C_b$, depending only on the load resistance $R_0$ and on the geometrical factors b and r .

In the high frequency regime the asymptotic response is purely resistive, i.e. the electrode voltage is in phase and proportional to the beam current. The transfer impedance scales with the inverse of the button capacitance and depends on the same geometrical factors above, but not on the value of $R_0$.

From the above considerations one can identify by which means it is possible to shape the response in a given frequency region. For example, by increasing the value of the load resistor, the corner frequency $\omega_1$ moves towards a lower value, extending the low-frequency response. The high frequency response is not affected as long as the capacitance value is the same. In fact, when dealing with long bunches, sometimes the load to electrostatic monitors is replaced by a high-impedance (cathode) follower mounted very close to the vacuum feedthrough, so to minimize any parasitic capacitance which spoils the high frequency response.

In the high frequency region the response can be enhanced by reducing the capacitance. The drawback is that the corner frequency $\omega_1$ moves towards a higher value.

The modulus of the transfer impedance

$$\left| Z_b(\omega) \right| = \phi R_0 \left( \frac{\omega_1}{\omega_2} \right) \frac{\omega/\omega_1}{\sqrt{1+\left(\omega/\omega_1\right)^2}} \tag{4}$$

scales as $r^2$. So, a bigger button radius would be preferable to get higher sensitivity at all frequencies.

In summary, the overall response can be enhanced by increasing the electrode surface, while an increase of capacitance leads to reduced response at high frequency and vice versa; the low frequency corner of the differentiator response can be reduced by increasing the value of the load resistor.

However, it must be pointed out that these parameters are not independent from each other: for example increasing the radius could correspond to a linear or quadratic increase of the capacitance, according to the specific design.

For the sake of example, the plot of Fig. 1 shows how the modulus of the impedance is affected if we double the button radius or the load resistance or halve the capacitance.
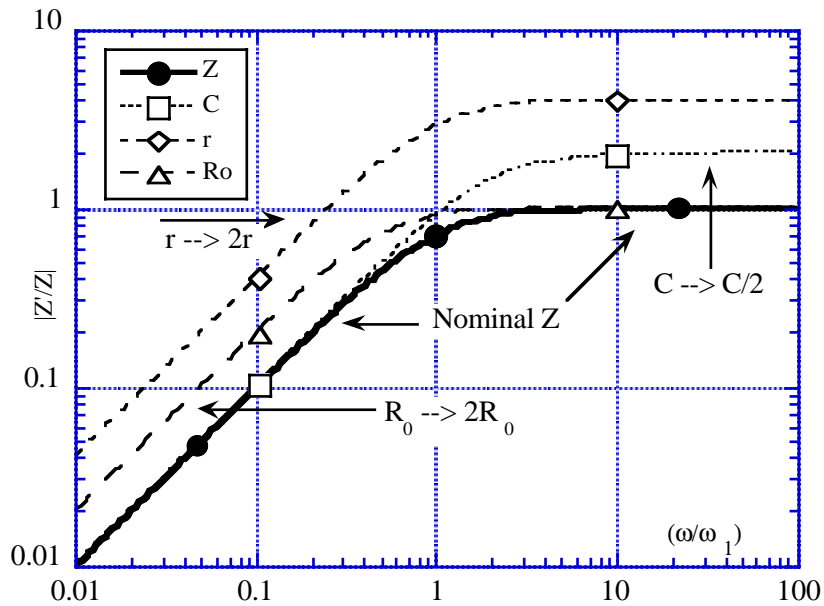


Fig. 1 - Comparison of the impedance behavior vs. large variations of r, $R_0$ and $C_b$.

On the other hand, following the arguments of [2, Appendix ], one can verify that the long wavelength component of the longitudinal coupling impedance can be written as:

$$Z_l(\omega) = \phi \left( \frac{\omega_1}{\omega_2} \right) Z_b , \tag{5}$$

i.e.: it scales as $r^4$. This puts a limit on the button radius.

We should also remark here that the expression (5) underestimates the coupling impedance, since it takes into account only that part of fields contributing to the output signal formation. In fact, some modes, which do not dissipate their power in the external termination, have been found with MAFIA [3-5]. The first one is the mode of TE-11 type, establishing around the electrodes. This mode has a wavelength close to the mean perimeter of the annular cut created by the button and beam pipe walls:

$$\lambda_1 = 2\pi \left[ \frac{r + (r+w)}{2} \right] \qquad (6)$$

where w is the width of the annular cut. In order to avoid high power losses in the button BPM, one should push the frequency of the first parasitic mode toward higher frequencies, possibly beyond the bunch spectrum, therefore, again, a smaller button radius is needed.

At low frequencies an additional contribution of the annular cut to the coupling impedance can be estimated analytically [6]:

$$Z_{l\,cut}(\omega) = j \frac{Z_0 \omega (r+w)^3}{8cb^2 \left\{ \ln\left[ 32(r+w)/w \right] - 2 \right\}} \qquad (7)$$

where $Z_0$ is the free space impedance. Here we find again a very strong dependence of the coupling impedance on the button radius. In the case of a thick button (w $\ll$ t, where t is the button thickness), the result of eq. (7) has to be multiplied by a factor of ~ 0.56. This contribution turns out to be the most significant at low frequency for our design.

The above considerations were taken into account in order to design a button with the necessary transfer impedance and possibly low coupling impedance. The proposed design is shown in Fig. 2. The button itself has a radius r of 7.5 mm and a thickness t of 3 mm, the annular gap w is 1 mm wide. The dielectric material with relative dielectric constant $\varepsilon_r$ ~ 5.2 is mainly used to fix the button and creates a short piece of transmission line with $R_0$ = 50 $\Omega$. A tapered transition has also the characteristic impedance of 50 $\Omega$ and provides matching between the button and the external coaxial connector.

In order to calculate the transfer impedance we apply expression (1), where the capacitance of the button to ground is estimated as that of a short coax formed by the button and the beam pipe inner walls (the matched part of the electrode does not contribute to the signal formation):

$$C_b \approx \frac{2\pi\varepsilon_0}{\ln\left( \frac{r+w}{r} \right)} t = 1.33 \text{ pF} . \qquad (8)$$

This gives a corner frequency $\omega_1/2\pi$ ~ 2.4 GHz and a high frequency limit |Z| ~ 1.6 $\Omega$. However, the parasitic capacitance between the upper and lower surfaces of the button and the beam pipe wall can substantially influence the final result. More precise numerical calculations are given in Section 2.

According to (6), the frequency of the first parasitic mode TE-like mode is to be found at 5.97 GHz, which is far beyond the bunch spectrum in DA$\Phi$NE (the bunch spectrum roll-off is ~1.6 GHz at 3 cm rms bunch length). The final check of this is made in Section 3.

The low frequency imaginary part of the normalized coupling impedance Z/n, estimated with (7), is j$*$1.8$*10^{-3}$ $\Omega$ for all the 12 buttons and is quite acceptable from the bunch dynamics point of view.
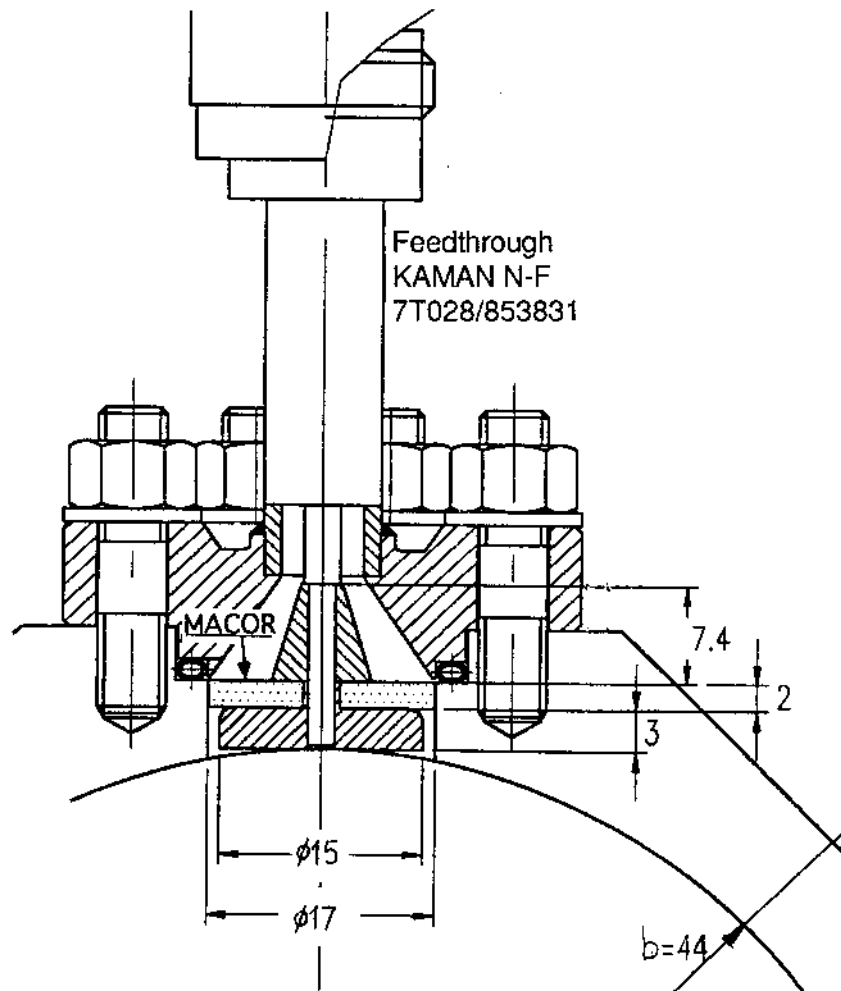
Fig. 2 - BPM button design.

## 2. Transfer Impedance

In order to estimate the transfer and coupling impedance of the button we have simulated with the HFSS code [7] the measurement method based on a coaxial wire put along with the beam tube [8, 9].

In Fig. 3 we show the geometry used in the simulations. The transfer impedance vs. frequency can be found from the values of the scattering matrix elements, directly obtained as HFSS output data, according to the following formula:

$$Z_b(\omega) = \frac{S_{31}(\omega)}{S_{21}(\omega)} \sqrt{Z_0' Z_0} \, , \qquad (9)$$

where $Z_0' = 130 \ \Omega$ and $Z_0 = 50 \ \Omega$ are respectively the characteristic impedances of the beam tube and output signal coaxial lines; $S_{21}$ and $S_{31}$ are the scattering parameters relating the two beam tube ports (ports 1 and 2) and one beam tube port to the button port (port 3), respectively.

Figure 4 shows the result obtained in the 0 - 6 GHz frequency range. In the working region the response of the device is sufficiently flat with a satisfactory value of the transfer impedance (0.43 Ω).
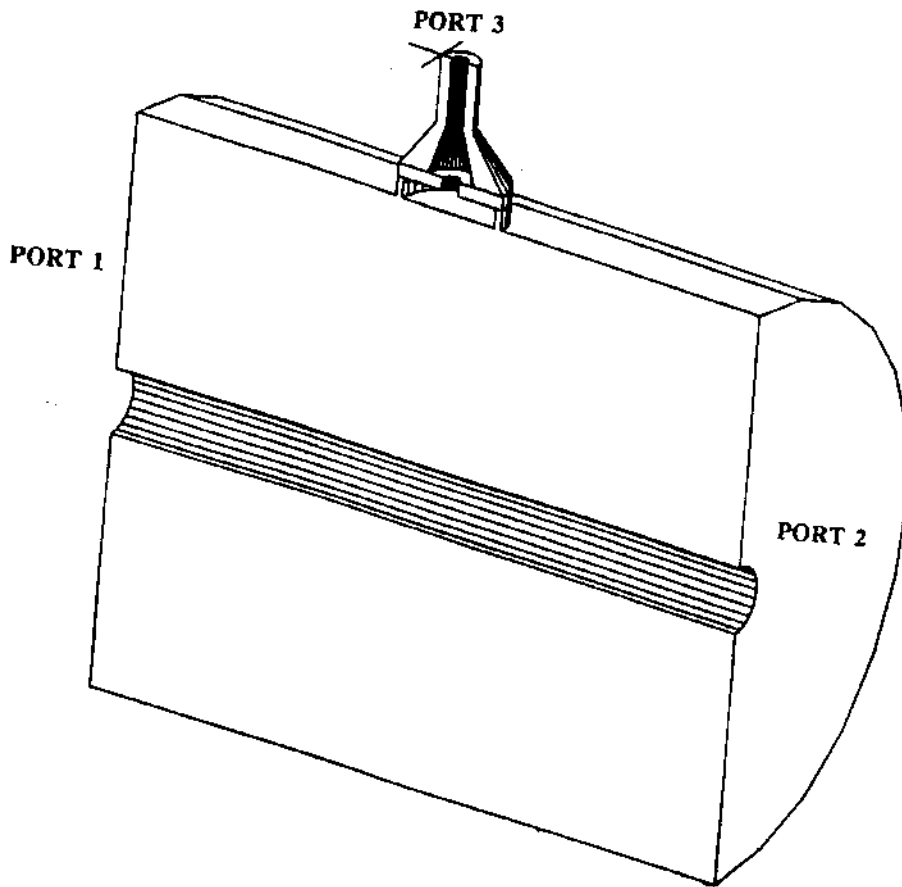
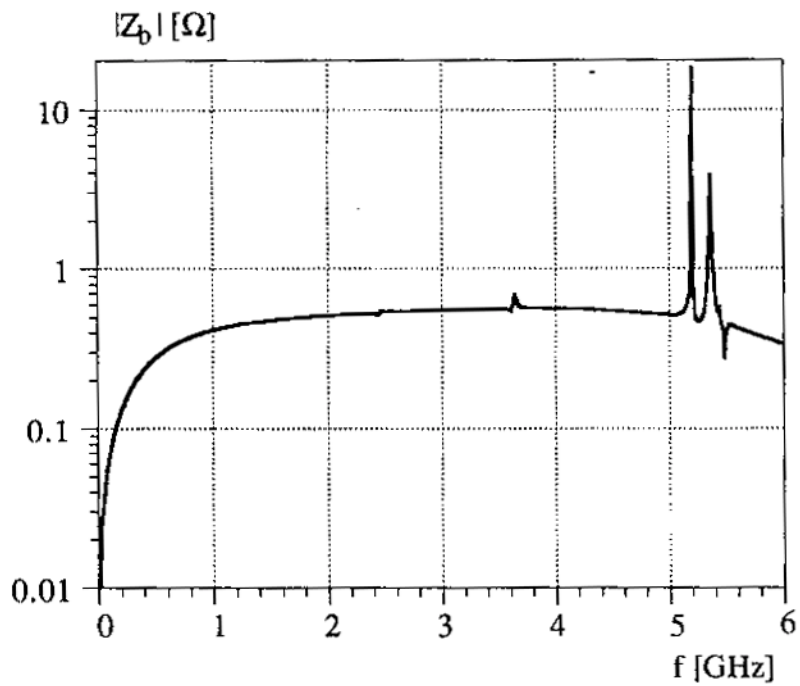Fig. 3 - HFSS input button geometry.

Fig. 4 - Button transfer impedance.

We remark that the simulated dependence of the transfer impedance on the frequency can be well fit by the analytical one, given by (4), with a value of the capacitance of the button to ground greater than twice that estimated with the crude approximation (8). We attribute this discrepancy to the parasitic capacitance between the upper and lower surfaces of the button and beam pipe walls, especially in the dielectric region. Indeed, only by smoothing the upper button corners, as shown in Fig. 2, we have gained about 17% in the transfer impedance.

## 3. Coupling Impedance

We use both MAFIA and HFSS simulation codes for the coupling impedance calculations. In order to get a preliminary information about the coupling impedance we trace the wake field behind a 5 mm long gaussian bunch over 1 m with MAFIA and then perform the Fourier transform of the wake.

Figure 5 shows the input BPM geometry for the MAFIA simulations. The output coaxial cable is rather long, > 0.5 m, in order to simulate 'quasi' matched conditions with the old MAFIA version, i.e.: the reflected wave from the short circuit termination at the end of the coaxial cable can not come back during all the time of the wake field tracing.
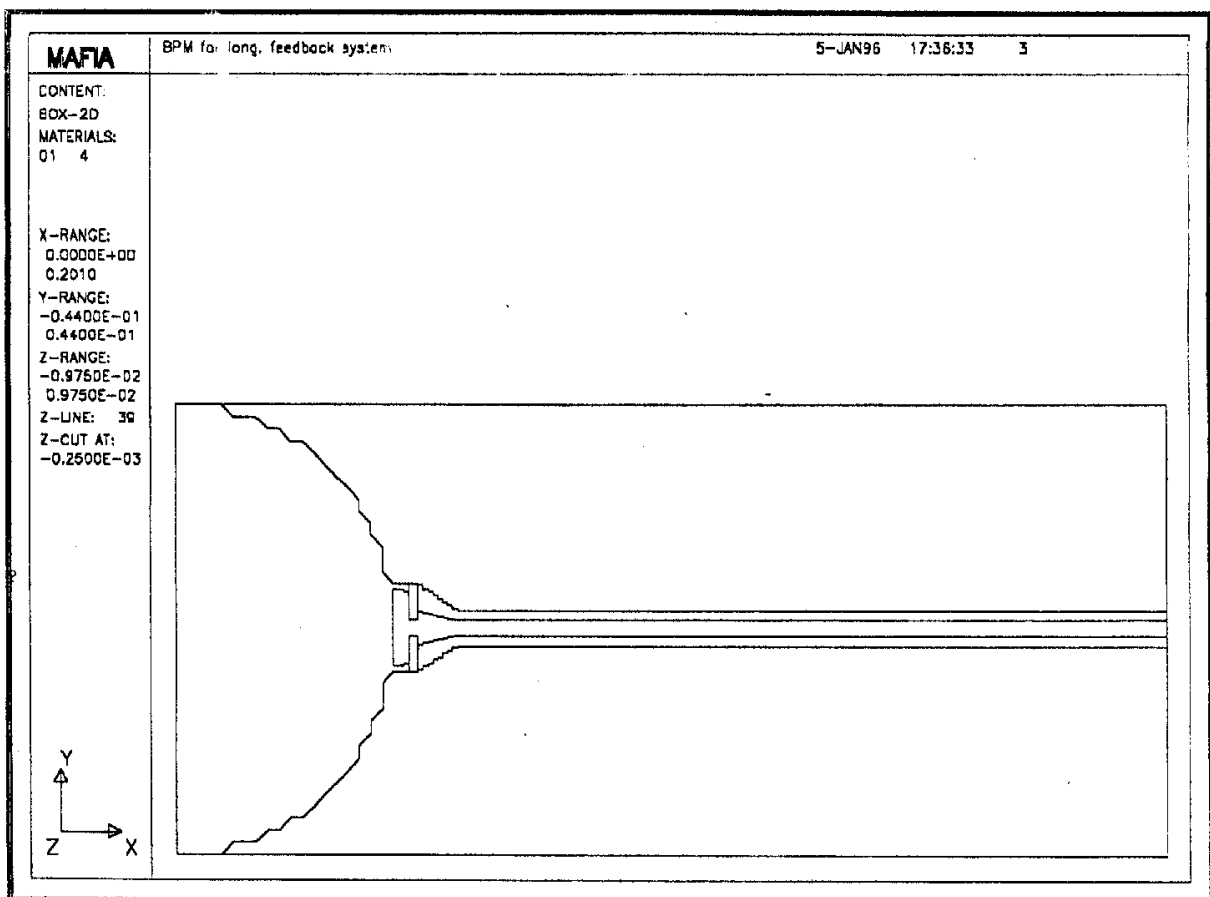


Fig. 5 - MAFIA input button geometry.

The real part of the resulting impedance is shown in Fig. 6. This impedance is artificially "broadened" because the Fourier transform is taken over the truncated wake field. Nevertheless, resonances can be clearly identified.

The first resonant peak is at 5.2 GHz and corresponds to the TE-110 mode trapped around the button. The electric field configuration of the mode as found by HFSS is presented in Fig. 7. The frequency of the mode is lower than the expected value of 5.97 GHz. We believe that this is due to the immediate presence of the dielectric material next to the button.
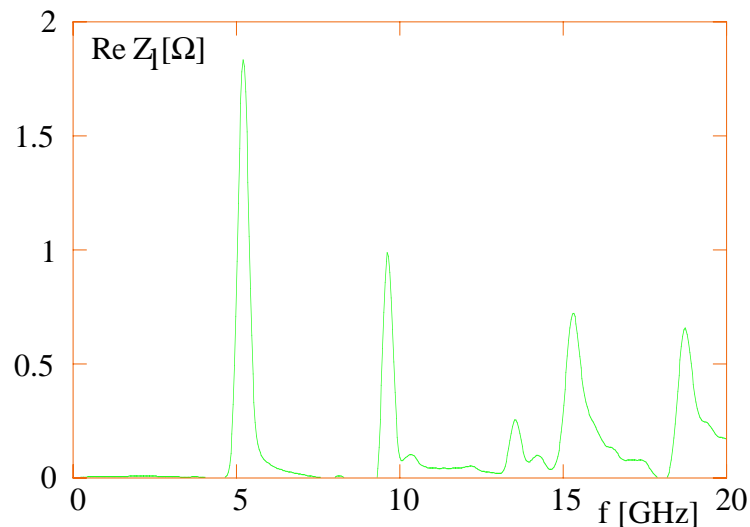


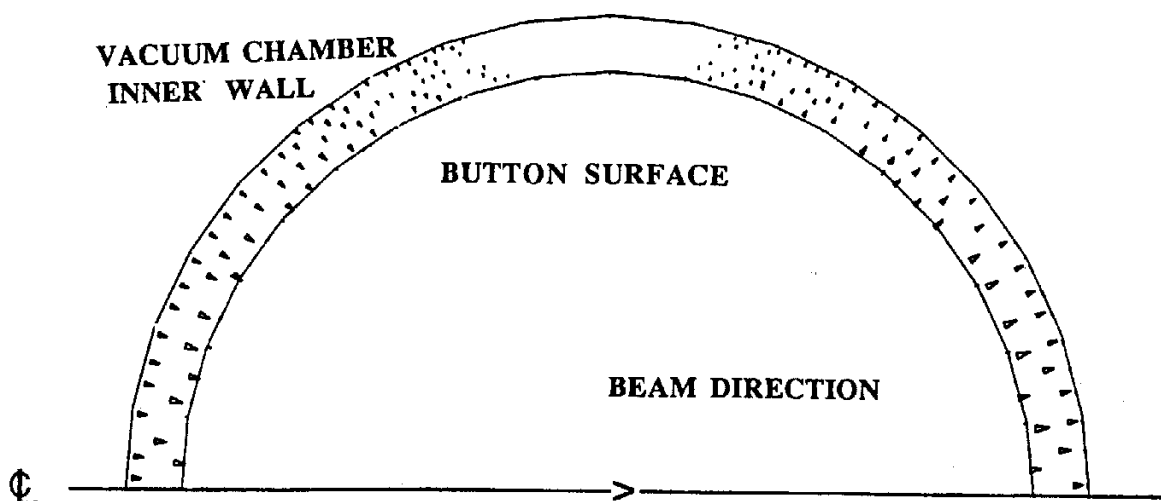Fig. 6 - Real part of the BPM coupling impedance (Fourier transform).



Fig. 7 - Electric field configuration of the first trapped mode (button top view).

The shunt impedance and the quality factor of the mode are respectively $R_s = 13$ $\Omega$ and $Q_L = 1570$ as found by post-processing the HFSS field solutions. The mode is not harmful for the multibunch instabilities since the calculated rise time is much longer than the radiation damping time in DAΦNE. We do not expect any substantial parasitic power losses due to this mode because it is situated beyond the 3 cm bunch frequency spectrum.

It is very important to calculate also the low frequency part of the coupling impedance (below the resonant region) because it can contribute to the potential well bunch lengthening and is responsible for the power losses in the external terminations. We again calculate the wake field with MAFIA, but for a gaussian bunch with $\sigma_z = 3$ cm. In this case the bunch spectrum covers the frequency range below the resonant region. As far as the low frequency impedance is rather flat the wake field decays very fast behind the bunch and the Fourier transform gives the exact value of the impedance. Figures 8 and 9 show the real and imaginary impedances at low frequencies, respectively.

We intentionally show the graph of the imaginary part using the linear scale to confirm that it grows linearly with frequency, i.e.: it is purely inductive. The estimated inductive impedance Im $(Z_l/n)$ is $0.8*10^{-3}$ $\Omega$, that is about a factor of 2 smaller than the value calculated analytically applying the expression (7) with the correcting factor 0.56.

The coupling impedance can be defined also by using the results of HFSS code obtained from the already discussed wire method measurement simulations. In this case we have [9]:

$$Z_l(\omega) = 2Z_0^{'}\left(\frac{1}{S_{21}(\omega)} - 1\right) \tag{10}$$

The resulting impedance is shown in Fig. 10 for frequency up to 6 GHz. The first strong mode at 5.2 GHz is the TE-110 mode observed also with MAFIA. The two small perturbations in the impedance at ~ 2.5 GHz and 3.8 GHz are close to the cutoff of the TM-01 and TM-11 waves in the beam pipe.
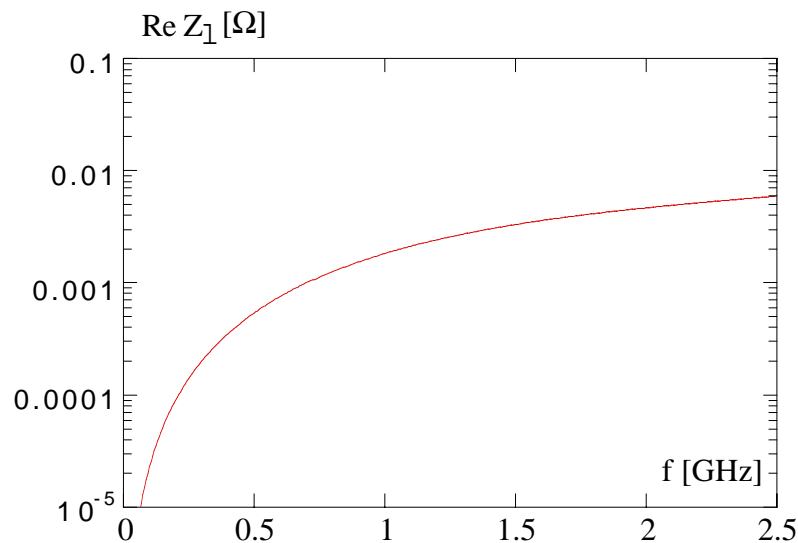


Fig. 8 - Real part of the BPM coupling impedance at low frequencies.
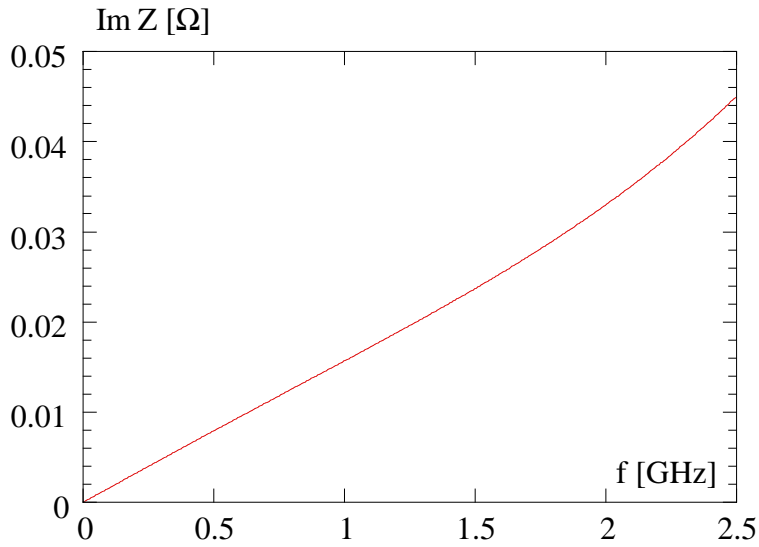
Im Z [Ω]

Fig. 9 - Imaginary part of the BPM coupling impedance at low frequencies.
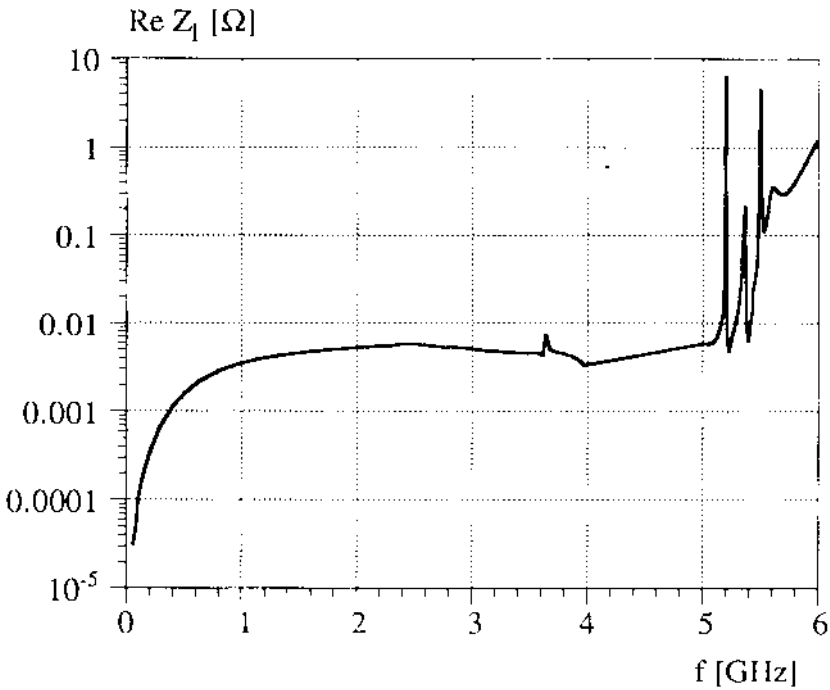
Re $Z_l$ [Ω]

Fig. 10 - Real part of the button coupling impedance as calculated by HFSS.

At low frequencies this dependence can be well approximated by the analytical formula (5) with $C_b$ =3.6 pF, as shown in Fig. 11. By comparing Figs. 8 and 11 we can conclude that the results of MAFIA and HFSS coincide pretty well.
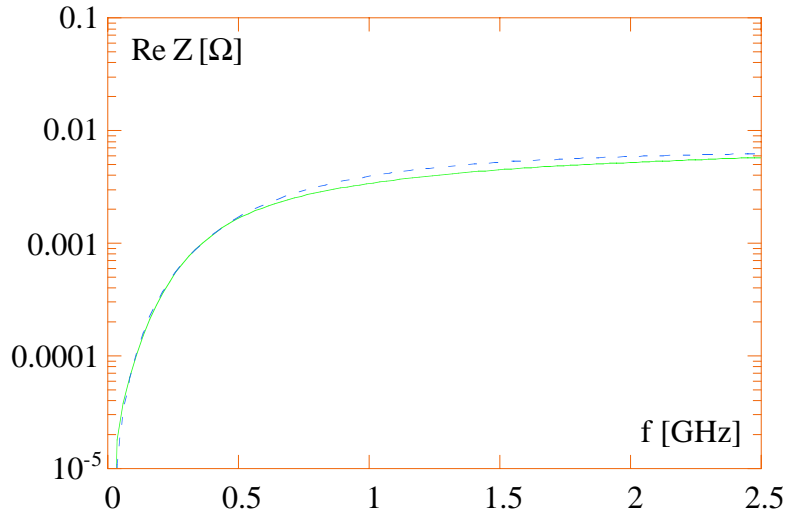


Fig. 11 - Long wavelength button coupling impedance: solid line - HFSS result; dashed line - analytical expression (5).

The power losses in the external termination can be easily estimated by applying the loss factor definition:

$$k_l = \frac{1}{\pi} \int\limits_0^\infty \mathbf{Re}\{Z_l(\omega)\} \exp\left[-(\omega\sigma_z / c)^2\right] d\omega .\qquad(11)$$

By substituting the analytical expression (5) with $C_b$ =3.6 pF for the impedance in (11) and performing the integration, we get:

$$k_l = \frac{R_0\phi^2(\omega_1 / \omega_2)^2}{\pi\sigma_z}\left\{\frac{\sqrt{\pi}}{2} - \frac{\pi}{2}\frac{\omega_1\sigma_z}{c}e^{(\omega_1\sigma_z/c)^2}\left[1 - \Phi\left(\frac{\omega_1\sigma_z}{c}\right)\right]\right\},\qquad(12)$$

where $\Phi$ is the error function.

From the analytically calculated impedance (5) the loss factor is $0.83*10^7$ V/C, while MAFIA gives practically the same value of $0.85*10^7$ V/C.

The long wavelength approximation of the impedance is broad band throughout the 3 cm bunch spectrum and we can neglect the multibunch enhancement factor in estimating the lost power, applying:

$$\langle P \rangle = k_l\langle I_0\rangle^2 T_0 n_b \qquad(13)$$

with $T_0$ the revolution time; $\langle I_0\rangle$ the bunch average current; $n_b$ the number of bunches in the ring. For the case of 120 bunches in DAΦNE the estimated power loss is $\langle P\rangle \sim 0.7$ W.

## 4. Conclusions

We have presented the proposed design of the DAΦNE BPM for the longitudinal feedback system. It has a transfer impedance of ~ 0.43 Ω at the working frequency which is higher than the necessary value of 0.3 - 0.4 Ω. The contribution of the button to the low frequency impedance is relatively small and is acceptable from the beam dynamics point of view. The first trapped HOM appears to be of TE-110 type and is situated beyond the bunch spectrum, therefore it does not contribute significantly to the power loss. Having rather small value of the shunt impedance neither it is dangerous to the multibunch instabilities. The estimated power loss in the external termination is less than 1 W.

## Acknowledgments

The mechanical design has been carried out skillfully by G. Sensolini and V. Lollo. We thank B. Spataro for useful discussions and for the help given in numerical simulations with MAFIA.

## References

[1] "DAΦNE Machine Project", Contributions to EPAC 94, London, 27/6 - 1/7 1994, LNF-94/055 (P).

[2] R. E. Shafer, "Characteristics of Directional Coupler Beam Position Monitors", IEEE Trans. on Nucl. Science, Vol. NS - 32, No.5, October 1985, pp. 1933 - 1937.

[3] R. Klatt, et. al., "MAFIA - A Three-Dimensional Electromagnetic CAD System for Magnets, RF Structures, and Transient Wake Field Calculations", SLAC report 303, 1986.

[4] C.-K. Ng, et. al., "Simulation of PEP - 2 Beam Position Monitors", SLAC - PUB - 95 - 6899, May 1995.

[5] T. Obina, et. al., " Damped Button Electrode for B - Factory BPM System", KEK Preprint 95 - 41, May 1995, A.

[6] S. S. Kurennoy, "Polarizabilities of an Annular Cut and Coupling Impedances of Button - Type Beam Position Monitors", presented at the 16th IEEE PAC95 and ICHEA, Dallas, Texas, May 1 - 5, 1995; e - Print Archive: acc - phys/9504003.

[7] Hewlett - Packard Co, "HFSS, The High Frequency Structure Simulator HP85180A™".

[8] W. Barry, "A General Analysis of Thin Wire Pickups for High Frequency Beam Position Monitors", Nucl. Instr. and Methods in Phys. Research A301 (1991), pp. 407 - 416.

[9] F. Caspers, "Bench Methods for Beam - Coupling Impedance Measurement", Proc. of a Topical Cource Held by the Joint US - CERN School on Particle Accelerators at Hilton Head Island, South Carolina, USA 7 -14 November 1990, Springer - Verlag.

[10] A. Papoulis: "The Fourier Integral and its Applications", Mc Graw-Hill Book Company, inc. (1962).

## APPENDIX

## The Long Wavelength Transfer and Coupling Impedance

The fraction of image current $\Delta i_b$ intercepted by a button electrode of a radius r is given by:

$$\Delta i_b = iF \frac{S_b}{S_t} , \qquad (A.1)$$

where i  is the bunch current, F is a form factor depending on the geometry of the beam pipe and on the button position and size, $S_b$ is the button area, $S_t$ is the total area of vacuum chamber of the same length as that of the button .

In a circular vacuum chamber of a radius b the image current is distributed uniformly over the beam pipe walls and the form factor F is equal to 1. In this case the intercepted current fraction is easily calculated:

$$\Delta i_b = i \frac{\pi r^2}{(2\pi b)2r} = i \frac{r}{4b} . \qquad (A.2)$$

In this paper we call the factor $\phi = r/4b$ the *coverage factor*.

The usual equivalent circuit representation of the ordinary button pick-up is a current generator of the same value of the current intercepted fraction $\Delta i_b$ , shunted by the electrode capacitance to ground $C_b$ (see Fig. A.1).



i(t)        $-\phi$ i(t)                Cb        Vb
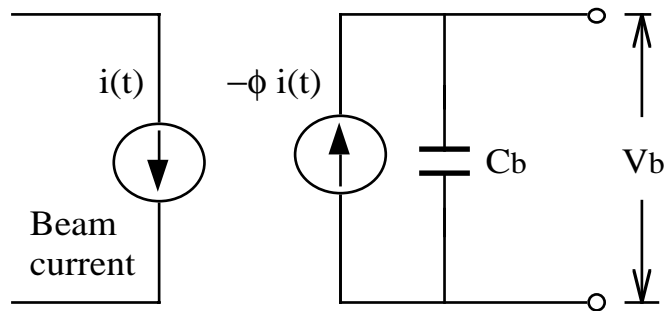
Beam
current

Fig. A.1 - Button equivalent circuit representation.

The voltage induced at the button (no load) can be written as:

$$V_b = \frac{1}{C_b} \int \Delta i_b \, dt . \qquad (A.3)$$

If the bunch is longer than the button radius we have:

$$V_b \cong \frac{1}{C_b} \Delta i_b \frac{2r}{c} = i \frac{r^2}{2bc} \frac{1}{C_b},$$ (A.4)

where c is the light velocity. Clearly, the equivalence (A.4) is always fulfilled for wavelengths much longer than the button size.

Now, let us rearrange the above equivalent scheme into a scheme with the voltage generator, presented in Fig. A.2.
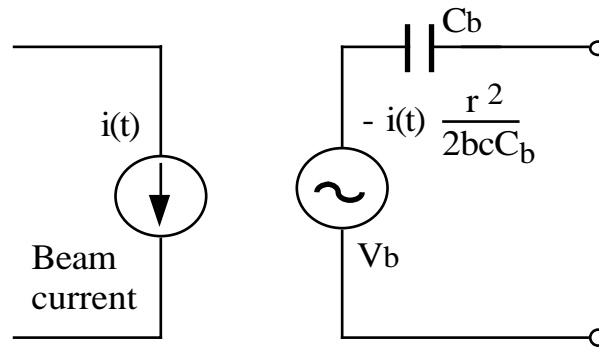


Fig. A.2 - Button equivalent circuit as an unloaded voltage generator.

The button is now terminated into the resistor $R_0$ via a coaxial cable with the characteristic impedance $Z_0 = R_0$. The corresponding equivalent scheme is shown in Fig. A.3.
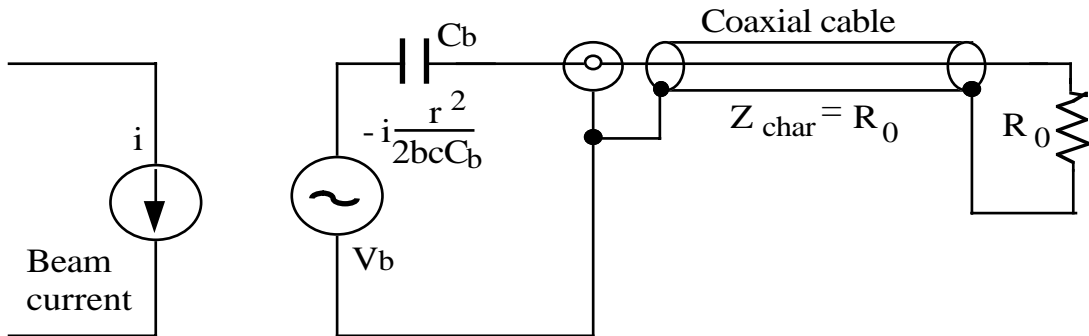


Fig. A.3 - Terminated button equivalent circuit.

In the frequency domain, the voltage at the termination load $R_0$ is given by:

$$V_o(\omega) = V_b(\omega) \frac{R_0}{R_0 + 1/j\omega C_b} = I(\omega) \frac{r^2}{2bc} \frac{1}{C_b} \frac{j\omega R_0 C_b}{1 + j\omega R_0 C_b}.$$ (A.5)

Here $V_0(\omega)$ and $I(\omega)$ are the spectral densities of the load voltage $V_0(t)$ and beam current $i(t)$, respectively. Then, according to the definition, the transfer (signal) impedance is given by:

$$Z_b(\omega) \equiv \frac{V(\omega)}{I(\omega)} = R_0 \frac{j\omega r^2/2bc}{1 + j\omega R_0 C_b} \; . \tag{A.6}$$

We now define $\omega_1 = 1/R_0 C_b$ and $\omega_2 = c/2r$ and re-write (A.6) as:

$$Z_b(\omega) = \phi R_0 \left(\frac{\omega_1}{\omega_2}\right) \frac{j\omega/\omega_1}{1 + j\omega/\omega_1} \; ,$$

$$\mathbf{Re}\{Z_b(\omega)\} = \phi R_0 \left(\frac{\omega_1}{\omega_2}\right) \frac{(\omega/\omega_1)^2}{1 + (\omega/\omega_1)^2} \quad , \quad \mathbf{Im}\{Z_b(\omega)\} = \phi R_0 \left(\frac{\omega_1}{\omega_2}\right) \frac{(\omega/\omega_1)}{1 + (\omega/\omega_1)^2} \quad .$$

$$\tag{A.7}$$

It is worth noting that the electrode itself can be regarded as forming a short piece of transmission line with the vacuum chamber. In a lossless transmission line (characteristic impedance $= Z_c$) of a given length, this general relation between the line length and the total capacity $C_{line}$ holds:

$$Z_c C_{line} = \frac{\text{line length}}{\text{propagation speed}} \; .$$

The propagation speed is $c$ in the absence of dielectric material. If the electrode characteristic impedance is matched to $R_0$ and no dielectric is present between the electrode and the vacuum chamber, then $R_0 C_b \sim$ electrode length/$c$ , or $\omega_1 \sim \omega_2$.

The frequency behavior of the real and imaginary part of the transfer impedance is shown in Fig. A.4.
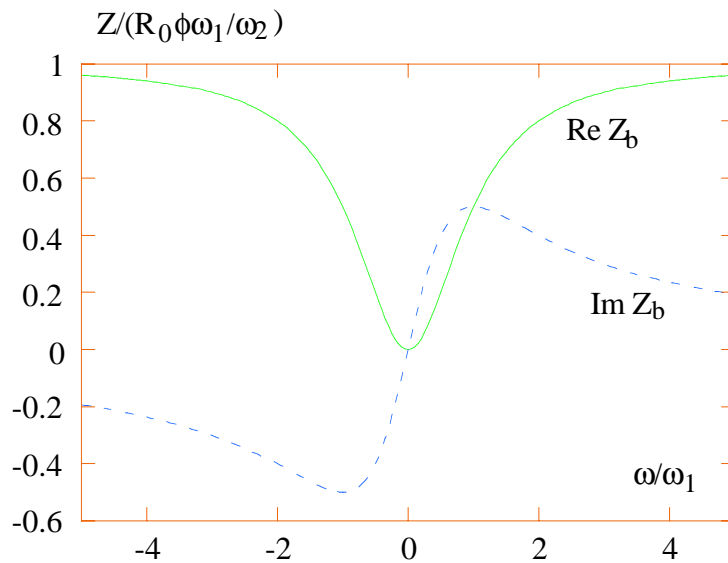


Fig. A.4 Real and imaginary parts of the BPM transfer impedance.

In order to get the coupling impedance, we calculate the average power dissipated at the external termination $R_0$ [2]:

$$\langle P(\omega) \rangle = \frac{1}{2}|V_0|^2 \frac{1}{R_0} = \frac{1}{2}|I|^2 R_0 \, \phi^2 \left(\frac{\omega_1}{\omega_2}\right)^2 \frac{(\omega / \omega_1)^2}{1 + (\omega / \omega_1)^2} \, . \tag{A.8}$$

This power is provided by the beam and can be written also as:

$$\langle P(\omega) \rangle = \frac{1}{2}|I|^2 \, \mathbf{Re}\{Z_l(\omega)\} \, , \tag{A.9}$$

where $Z_l$ is the longitudinal coupling (parasitic) impedance.

By comparing (A.8) and (A.9) we get the expression for the real part of the longitudinal coupling impedance:

$$\mathbf{Re}\{Z_l(\omega)\} = R_0 \, \phi^2 \left(\frac{\omega_1}{\omega_2}\right)^2 \frac{(\omega / \omega_1)^2}{1 + (\omega / \omega_1)^2} \, . \tag{A.10}$$

As it can be easily observed, the coupling impedance has the same frequency behavior as the transfer impedance $Z_b$ but for the factor $\phi(\omega_1/\omega_2)$.

In a causal system the real and imaginary parts of the Fourier transform of the pulse response function are related to each other by a Hilbert transforms pair (see[2],[10]):

$$\mathbf{Im}\{Z(\omega)\} = -\frac{1}{\pi} \int_{-\infty}^{\infty} \frac{\mathbf{Re}\{Z(\omega')\}}{\omega - \omega'} \, d\omega' \, ,$$

$$\tag{A.11}$$

$$\mathbf{Re}\{Z(\omega)\} = \frac{1}{\pi} \int_{-\infty}^{\infty} \frac{\mathbf{Im}\{Z(\omega')\}}{\omega - \omega'} \, d\omega' \, .$$

From the knowledge of the real part of the coupling impedance (A.10), the imaginary part can thus be calculated by applying (A.11):

$$\mathbf{Im}\{Z_l(\omega)\} = R_0 \phi^2 \left(\frac{\omega_1}{\omega_2}\right)^2 \frac{\omega / \omega_1}{1 + (\omega / \omega_1)^2} \, . \tag{A.12}$$

Like in case of the real part, we again find a similar frequency behavior of the imaginary part of the coupling and transfer impedances except for the same constant factor $\phi(\omega_1/\omega_2)$. From the above arguments we conclude that

$$Z_l = \varphi\left(\frac{\omega_1}{\omega_2}\right) Z_b \, . \tag{A.13}$$